PHYSICAL REVIEW D **81,** 043007 (2010)

Obtaining supernova directional information using the neutrino matter oscillation pattern

Kate Scholberg,[1] Armin Burgmeier,[2] and Roger Wendell[1]
[1]*Department of Physics, Duke University, Durham, North Carolina 27708 USA*
[2]*Universität Karlsruhe, 76128 Karlsruhe, Germany*
(Received 20 October 2009; published 10 February 2010)

A nearby core collapse supernova will produce a burst of neutrinos in several detectors worldwide. With reasonably high probability, the Earth will shadow the neutrino flux in one or more detectors. In such a case, for allowed oscillation parameter scenarios, the observed neutrino energy spectrum will bear the signature of oscillations in Earth matter. Because the frequency of the oscillations in energy depends on the path length traveled by the neutrinos in the Earth, an observed spectrum also contains information about the direction to the supernova. We explore here the possibility of constraining the supernova location using matter oscillation patterns observed in a detector. Good energy resolution (typical of scintillator detectors), well-known oscillation parameters, and optimistically large (but conceivable) statistics are required. Pointing by this method can be significantly improved using multiple detectors located around the globe. Although it is not competitive with neutrino-electron elastic scattering-based pointing with water Cherenkov detectors, the technique could still be useful.

DOI: 10.1103/PhysRevD.81.043007 PACS numbers: 14.60.Pq, 95.55.Vj, 97.60.Bw

I. INTRODUCTION

The core collapse of a massive star leads to emission of a short, intense burst of neutrinos of all flavors. The time scale is tens of seconds and the neutrino energies are in the range of a few tens of MeV. Several detectors worldwide, both current and planned for the near future, are sensitive to a core collapse burst within the Milky Way or slightly beyond [1]. Future very large supernova-sensitive neutrino detectors, including water Cherenkov detectors of the 100 kton or greater scale (e.g., a water Cherenkov detector in South Dakota [2], Hyper-K [3], and MEMPHYS [4]), and scintillator detectors of the 10 kton or greater scale (e.g., LENA [5] and HanoHano [6]) are planned for the next few decades.

The first electromagnetic radiation is not expected to emerge from the star for hours, or perhaps even a few days. Therefore any directional information that can be extracted from the neutrino signal will be advantageous to astronomers who can use such information to initiate a search for the visible supernova. We note that not every core collapse may produce a bright supernova: some supernovae may be obscured, and some core collapses may produce no supernova at all, in which case directional information will aid the search for a remnant.

The possibility of using the neutrinos themselves to point back to the supernova has been explored in the literature [7,8]. Triangulation based on relative timing of neutrino burst signals was also considered in [7]; however available statistics, as well as considerable practical difficulties in prompt sharing of information, makes time triangulation more difficult. Leaving aside the possibility of a TeV neutrino signal [8] (which would likely be delayed), the most promising way of using the neutrinos to point to a supernova is via neutrino-electron elastic scattering: neutrinos interacting with atomic electrons scatter their targets within a cone of about 25° with respect to the supernova direction. The quality of pointing goes as $\sim N^{-1/2}$, where N is the number of elastic scattering events. In water and scintillator detectors, neutrino-electron elastic scattering represents only a few percent of the total signal, which is dominated by inverse beta decay $\bar{\nu}_e + p \rightarrow n + e^+$, for which anisotropy is weak [9]. Furthermore the directional information in the elastic scattering signal is available only for water Cherenkov detectors, for which direction information is preserved via the Cherenkov cone of the scattered electrons. Taking into account the near-isotropic background of nonelastic scattering events [8], a Super-K-like detector [10] (22.5 kton fiducial volume) will have 68% (90%) C.L. pointing of about 6° (8°) for a 10 kpc supernova; this could improve to $<1°$ for next-generation Mton-scale water detectors. Long string water detectors [11] do not reconstruct supernova neutrinos event by event and so cannot use this channel for pointing. Scintillation light is nearly isotropic and so scintillation detectors have very poor directional capability, although there is potentially information in the relative positions of the inverse beta decay positron and neutron vertices [12], and some novel scintillator directional techniques are under development [15].

We consider here a new possibility: detectors with sufficiently good energy resolution will be able to obtain directional information by observing the effects of neutrino oscillation on the energy spectrum of the observed neutrinos, assuming that oscillation parameters are such that matter oscillations are present. Although not competitive with elastic scattering, some directional information can be obtained even in a single detector (unlike for time triangulation). Combinations of detectors at different locations around the globe may yield fairly high quality information.

In Sec. II we describe the basic concept. In Sec. III A we first examine results for the case of perfect energy resolution, for single and multiple detectors. In Sec. III B we obtain results for more realistic water and scintillator detector resolutions, for single and multiple-detector configurations, and we briefly examine incorporation of relative timing information. In Sec. IV we discuss possible uncertainties and potential improvements of the technique, and in Sec. V we summarize the overall results.

II. DETERMINING THE DIRECTION WITH EARTH MATTER EFFECTS

Supernova neutrinos traversing the Earth's matter before reaching a detector will experience matter-induced oscillations, depending on the values of the Maki-Nakagawa-Sakata matrix parameters [16–21]. Whether or not there will be an Earth matter effect depends on currently-unknown mixing parameters, θ_{13} and the mass hierarchy: matter oscillation will occur for both ν_e and $\bar{\nu}_e$ for values of $\sin^2\theta_{13} \lesssim 10^{-5}$, for normal but not inverted hierarchy; if θ_{13} is relatively large, $\sin^2\theta_{13} \gtrsim 10^{-3}$, then matter oscillation occurs for $\bar{\nu}_e$ but not ν_e for either hierarchy [22,23]. The frequency of the oscillation in L/E, where E is the neutrino energy and L is the neutrino path length in Earth matter, depends on now fairly well-known mixing parameters. Therefore, the oscillation pattern in neutrino energy E measured at a single detector contains information about the path length L traveled through the Earth matter. If the path length L is known, one knows that supernova is located somewhere on a ring on the sky corresponding to this path length. If another path length is measured at a different location on the globe, the location can be further constrained to the intersection of the allowed regions.

A Fourier transform of the inverse-energy distribution [16] of the observed neutrinos will yield a peak if oscillations are present. References [16,17] explore the conditions under which peaks are observable with a view to obtaining information about the oscillation parameters. The authors assume that the direction of the supernova, and hence the path length through the Earth, is known. Here we turn the argument around: we assume that oscillation parameters are such that the matter effects do occur and can be identified, and that enough is known about Maki-Nakagawa-Sakata parameters to extract information about L and hence about supernova direction from the data. A similar idea to determine possible geo-reactor location from the oscillated spectrum was explored in Ref. [24]. We note that by the time a nearby supernova happens, the hierarchy and whether θ_{13} is large or small may in fact be known from long-baseline and reactor experiments. With reasonably high probability [25], the Earth will shadow the supernova in at least one detector. We note that *lack* of observation of a matter peak in the inverse-energy transform (assuming there should be one) gives some direction information as well: if no peak is present, one can infer that the supernova is overhead at a given location. If the hierarchy and value of θ_{13} are already known with sufficient precision at the time of the supernova, we will know in advance whether or not a peak in the k distribution should appear; otherwise, its appearance for at least one detector location may answer the question.

III. EVALUATION OF THE CONCEPT IN IDEALIZED SCENARIOS

To evaluate the general feasibility of this concept we make several simplifying assumptions. We consider only inverse beta decay in large water Cherenkov and liquid scintillator detectors (we ignore the presence of other interactions, which should be a small correction; some of them can be tagged) [26]. We will first consider a detector with perfect energy resolution, and then consider resolutions more typical of real water Cherenkov and scintillator detectors.

We borrow some of the assumptions and notation of Ref. [16]. We assume a neutrino interaction cross section proportional to E^2, perfect detection efficiency above threshold, and no background. We assume a "pinched" neutrino spectrum of the form:

$$F_0 = \frac{\phi_0}{E_0}\frac{(1+\alpha)^{1+\alpha}}{\Gamma(1+\alpha)}\left(\frac{E}{E_0}\right)^{\alpha} e^{-(\alpha+1)(E/E_0)} \qquad (1)$$

where E_0 is the average neutrino energy. We choose parameters $\alpha = 3$, average energies for the flavors $E_{\bar{\nu}_e} = 15$ MeV and $E_{\bar{\nu}_x} = 18$ MeV, and $\frac{\phi_{\bar{\nu}_e}}{\phi_{\bar{\nu}_x}} = 0.8$. These parameters correspond to the "Garching" model [28]. We ignore for this study "spectral splits" (e.g., [29]) or other features which will introduce additional Fourier components. We assume that there are no nonstandard neutrino interactions or other exotic effects that modify the observed spectra.

The oscillation probabilities have been computed by a numerical solution of the matter oscillation equations [30] using these vacuum parameters and the full PREM Earth density model [31]. Between neighboring radial points in the model the matter density is taken to be constant such that the three-neutrino transition amplitude may be computed following the methods outlined in [32]. The final amplitude is the product of all amplitudes across the matter slices along the neutrino's trajectory. The initial flux of neutrinos is taken to arrive at the Earth as pure mass states such that the detection probability is taken according to the probability of a neutrino being $\bar{\nu}_e$ flavor when it reaches the detector. The oscillation parameters were chosen to be $\sin^2 2\theta_{12} = 0.87$, $\sin^2 2\theta_{13} = 0$, $\sin^2 2\theta_{23} = 1.0$, $\Delta m^2_{12} = 7.6 \times 10^{-5}$ eV^2, and $\Delta m^2_{23} = 2.4 \times 10^{-3}$ eV^2.

A. Perfect energy resolution

The spectrum of inverse beta decay events, integrated over time, is shown in Fig. 1. Figure 1 shows on the bottom

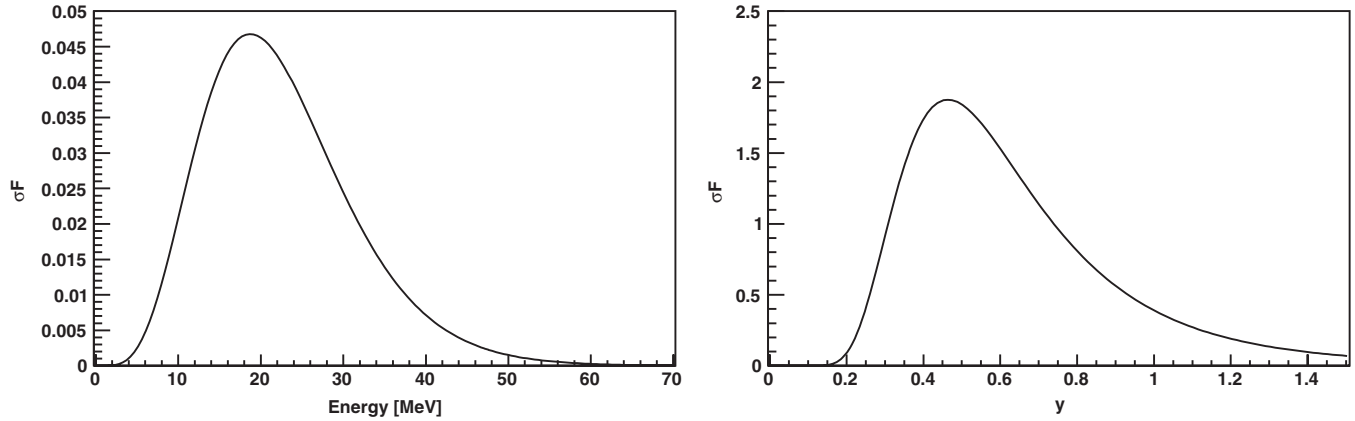

FIG. 1. Left panel: assumed neutrino event spectrum without oscillations. Right panel: inverse-energy distribution.

the ''inverse-energy'' spectrum, where the inverse-energy parameter y is defined as $y = \frac{12.5\ \mathrm{MeV}}{E}$. Figure 2 shows the Earth matter modulation of the spectrum, for $L = 6000$ km. Shown on the bottom is the modulation in inverse energy, for which the peaks are evenly spaced.

The Fourier transform of the detected inverse-energy spectrum is $g(k) = \int_{-\infty}^{\infty} f(y) e^{iky} dy$. The power spectrum $G_{\sigma F}(k) = |g(k)|^2$ assuming perfect energy resolution is shown in Fig. 3, for no matter oscillation on the top and for matter oscillation on the bottom, assuming path length $L = 6000$ km. The power spectra are generated from the

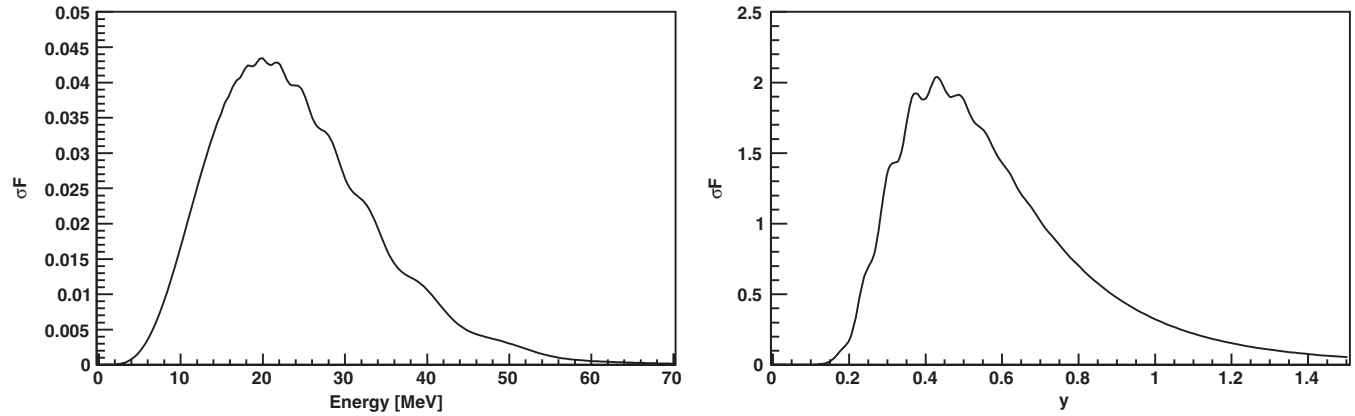

FIG. 2. Left panel: assumed neutrino event spectrum with matter oscillations for $L = 6000$ km. Right panel: inverse-energy distribution with matter oscillations.

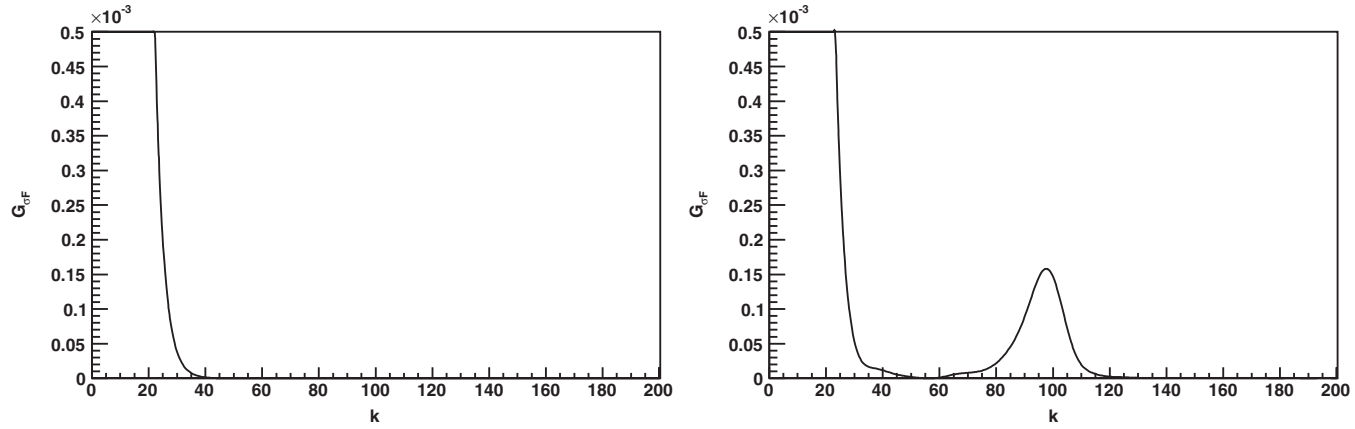

FIG. 3. Inverse-energy power spectrum without (left panel) and with (right panel) matter oscillations.

normalized inverse-energy distributions for which $\int_0^\infty \sigma F(y)dy = 1$. Thus the power spectra are normalized so that $G_{\sigma F}(0) = 1$. Figure 4 shows the power spectra for several values of L, illustrating how the peak moves to higher k values as the path length increases. For path lengths such that the neutrinos traverse the Earth core ($L >$ 10 700 km), additional peaks are present in the spectrum [17]. There is no observable peak for L less than about 2500 km, for which the neutrinos are no longer traversing much high-density matter.

Figure 5 shows now the effect of finite statistics, for a simulated supernova with 10 000 events and one with 60 000 events. The finite statistics result in a background for the main peak(s) in the power spectrum. For most of the following, we consider a rather optimistically large (but not unthinkable) 60 000 event signal, which would correspond to a supernova at a distance of about 5 kpc observed with a 50 kton detector.

1. Method for determining directional information

If one measures k_{peak}, the position of the largest peak in the power spectrum, for a supernova signal, one can in principle determine the path length traveled by the neutrino in the Earth. We use a simple Neyman construction method [33] to estimate the quality of directional information.

We first find the position of the largest peak in k as a function of path length L, assuming perfect energy resolution but finite statistics. To find the peak in the power spectrum, we first set a lower threshold of $k = 40$ and an upper threshold of $k = 210$. Below that threshold, the peak merges with the low k peak (corresponding to the unoscillated spectrum) and can no longer be identified. Peaks beyond $k = 210$ would correspond to distances greater than the diameter of the Earth. For each k within that range we then evaluate the integral from $k - \Delta k/2$ to $k + \Delta k/2$ which corresponds to the area under the peak. We take the k for which this value is highest as the peak in the spectrum. We choose $\Delta k = 4$. Even though Fig. 4 suggests that peaks can be wider than that, we found more fluctuation in the peak's position for higher Δk when taking finite energy resolution into account, especially for small distances ($L <$ 4000 km). Figure 6 shows that the value of k_{peak} is clearly correlated with path length L; for distances less than about 2000 km, for which the neutrinos do not undergo matter oscillations, it represents mainly random noise. The multiple peak structure for neutrinos passing through the core is clearly visible for $L > 10\,700$ km. We note that the height of the largest peak also contains information about L, as do the secondary peak positions, if such exist.

Given a particular measurement of k_{peak}, one can then determine a range of distances L allowed, making use of the Neyman construction shown in Fig. 7. To ensure contiguous regions in k we drop regions that contribute less than 3% to the final Neyman construction and increase existing regions instead so that the total covered area is 68% or 90%. The range in L values can then be mapped to an allowed region on the sky. We have checked explicitly that the statistical coverage is as expected.

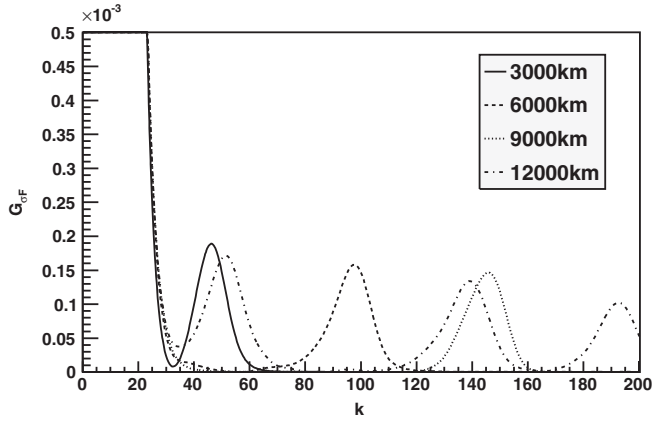

FIG. 4. Examples of inverse-energy power spectra for several path lengths.

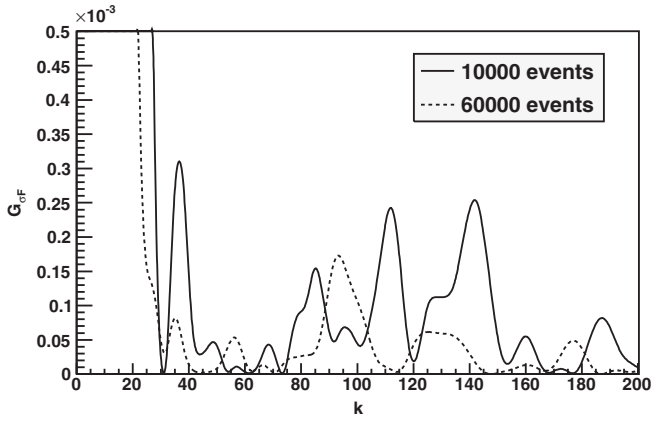

FIG. 5. Examples of inverse-energy power spectra for perfect energy resolution but finite statistics. Both lines show $L =$ 6000 km.

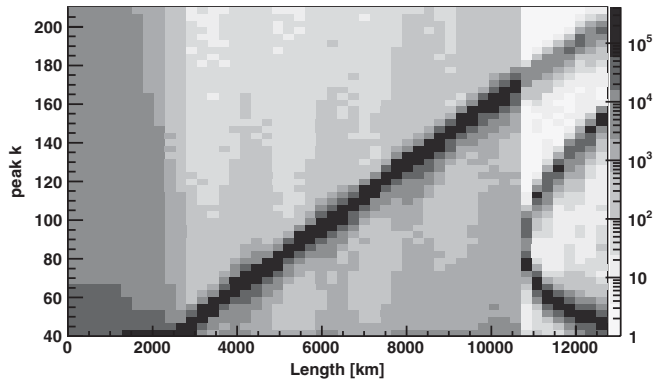

FIG. 6. Distribution of the position of the maximum peak in k as a function of matter-traversed path length L, assuming perfect energy resolution. There are 500 000 simulated supernovae per L, each with 60 000 events.

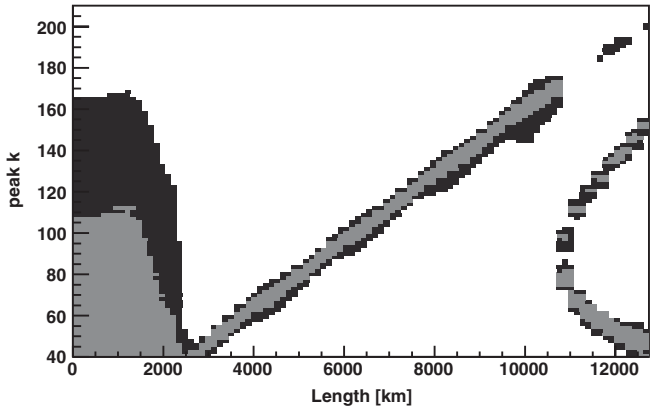

FIG. 7. Neyman construction for k_{peak} and L: for a given measured k_{peak} one reads off a range of allowed L values. The bright area shows the 68% confidence region and the dark area shows the 90% one.

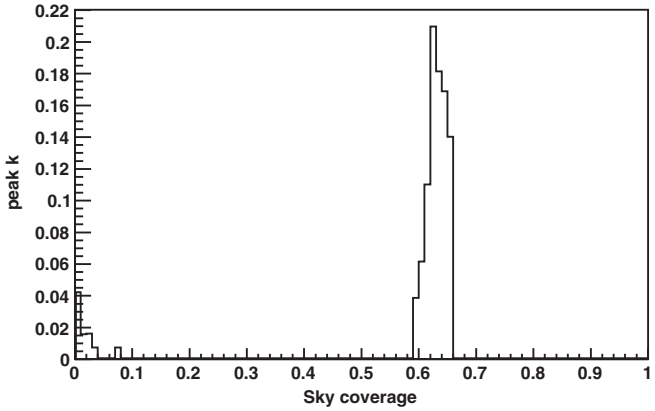

FIG. 9. Histogram of fractional sky coverages for the 90% C.L. region, assuming perfect energy resolution in a single detector, using k_{peak} information only, for the example configuration of Fig. 8.

Figure 8 shows an example Hammer projection sky map in equatorial coordinates showing 90% C.L. allowed regions for an assumed true supernova direction (indicated by a star) of R.A. $= 20^h$ and decl. $= -60°$ (occurring at 0:00 GMST), for assumed perfect energy resolution and statistics of 60 000 events.

Figure 9 shows the distribution of fractional sky coverage for perfect energy resolution. The distribution is bimodal, because the $L < 2500$ km possibility (corresponding to large fractional sky coverage) is often not excluded at 90% in the Neyman construction. Figure 10 shows the average sky coverage vs declination of the supernova, averaged over 24 h of right ascension, for a detector located in Finland (63.66°N, 26.04°E).

If we incorporate also information about the height of the largest peak h into a Neyman construction, for long path lengths we can remove the possibility of a short-path length overhead supernova, and improve the pointing quality significantly. Figure 11 shows the correlation between peak heights and L. Figures 8 (right) and 10 show the effect of incorporating this information. Subsequent plots will assume use of both power spectrum peak position and height information.

2. Combining detectors

Clearly, having several detectors around the globe observing the neutrino burst will improve the measurement. If each of the detectors could select a single L, an observation with two detectors would produce two allowed regions where the rings on the sky overlap, and a third observation would narrow it down to one spot. However because more than one L region may be allowed for a given detector, the combination can include multiple regions.

For the multiple-detector case, we make the Neyman construction for 100 000 randomly chosen $(k_1; h_1, k_2; h_2, \ldots)$-tuples only (with 100 bins in k_{peak} and height for each detector) in order to compute it in a reasonable amount of time. In this case the smoothing procedure described above is not applied.

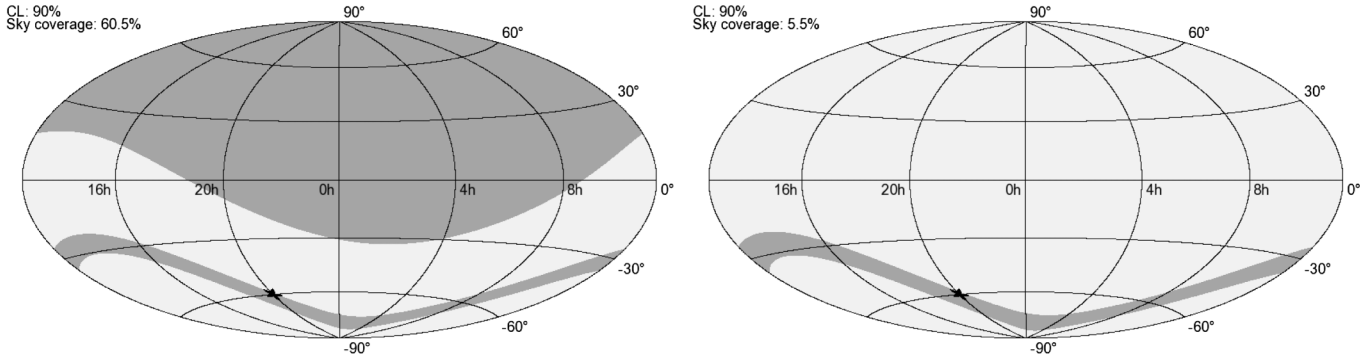

FIG. 8. Example Hammer projection sky maps in equatorial coordinates, showing 90% C. L. allowed regions on the sky for a supernova at the position indicated by a star. A 60 000 neutrino event signal measured in Finland with perfect energy resolution is assumed. The left plot shows the allowed region without taking into account peak height; the right plot takes into account peak height information.

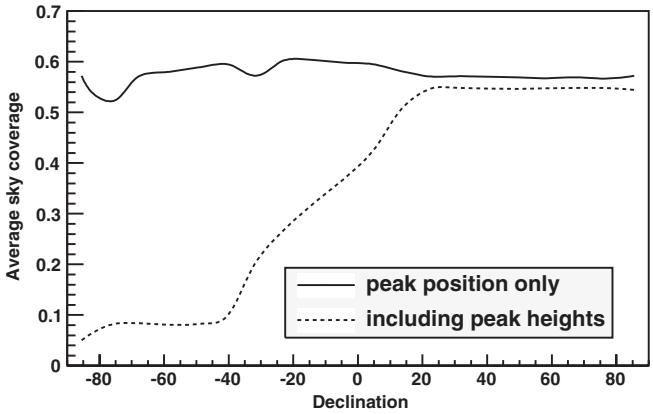

FIG. 10. Sky coverage averaged over right ascension as a function of declination, for a single detector with perfect energy resolution. The solid line takes into account the peak position only, whereas the dashed line includes also the height of the peak. In total, 83 500 supernovae, evenly distributed over declination, have been simulated for both lines.

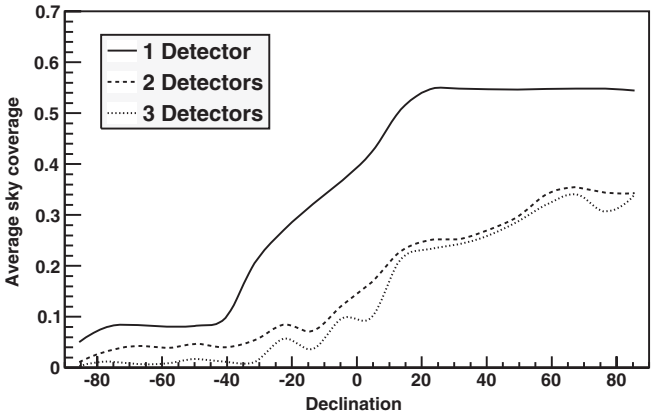

FIG. 13. Sky coverage averaged over right ascension as a function of declination, for one, two, and three detectors with perfect energy resolution. For one detector 83 500 supernovae have been simulated, for two detectors the number is 2630 and for three detectors it is 760.

Figure 12 shows example scenarios involving two and three detectors and Fig. 13 summarizes average quality as a function of declination. Clearly in this idealized situation, combined information is quite good, and the more detectors spread around the globe, the better.

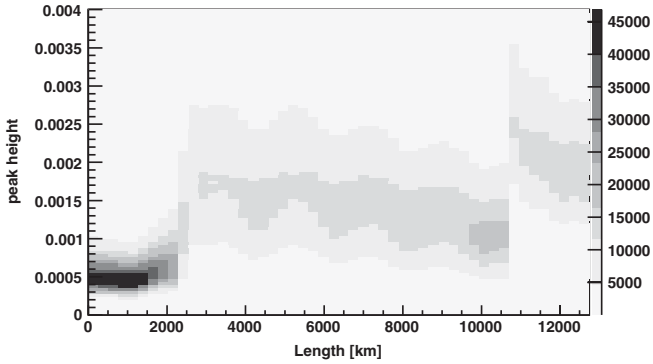

FIG. 11. Distribution of the heights of the maximum peak in k as a function of matter-traversed path length L, assuming perfect energy resolution. There are 500 000 simulated supernovae per L, each with 60 000 events.

B. More realistic detectors

Next we will assume a slightly more realistic situation. Imperfect energy resolution will tend to smear out the oscillation pattern and degrade the detectability of the peak in k. We estimate the effect of energy resolution by selecting events from the spectrum and smearing their energies according to a Gaussian of the prescribed width. The energy resolution functions used, the same as in Ref. [17], are shown in Fig. 14; one is characteristic of scintillator and one of water Cherenkov detectors. For water Cherenkov we assume a threshold of 5 MeV and for scintillator we assume a threshold of 1 MeV.

1. Water Cherenkov detectors

Figure 15 shows the distribution of k_{peak} and L for simulated supernovae in a detector with water-Cherenkov-like energy resolution. Figure 16 shows the same for scintillator.

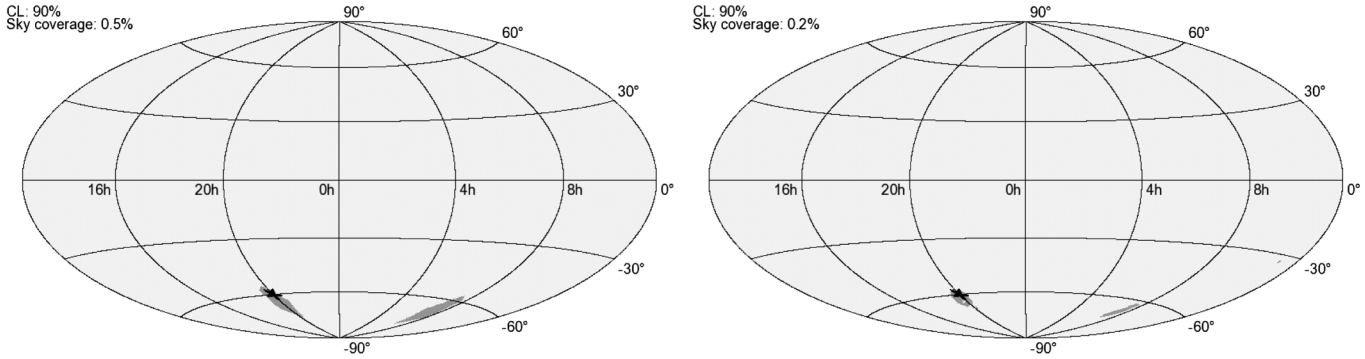

FIG. 12. Combined sky maps for detectors with perfect energy resolution. Left panel: Two detectors with 60 000 events each. Right panel: Three detectors with 60 000 events each.

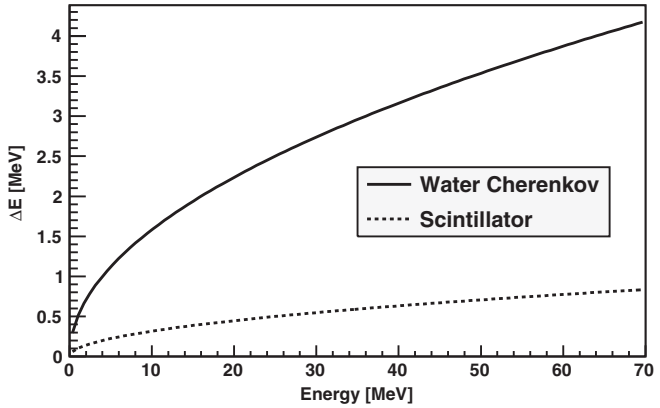

FIG. 14. Energy resolution functions used for water and scintillator. ΔE is the standard deviation σ of a Gaussian.

Clearly the water Cherenkov resolution smears the power spectrum information enough to preclude its use for this purpose; furthermore, far superior direction information will come from elastic scattering in a water Cherenkov detector. Therefore we will focus subsequent attention on scintillator detectors, which have significantly better energy resolution and weak intrinsic direct pointing capabilities.

2. Scintillator detectors

Existing and near-future scintillator detectors with supernova neutrino detection capabilities are KamLAND [34], LVD [35,36], Borexino [37], and SNO+ [38]; a 5 kton detector at Baksan [39] has also been proposed. These detectors are however probably too small to acquire the large statistics required for this technique. Future scintillator detectors of the tens of kton scale for which this technique could be feasible are LENA [5], to be sited in Finland, and the ocean-based HanoHano [6].

Figure 17 shows an example sky map for a scintillator detector located in Finland. Figure 18 shows average sky coverage vs declination for four examples of event statistics. Clearly at least a few tens of thousands of events are required for this technique to be useful.

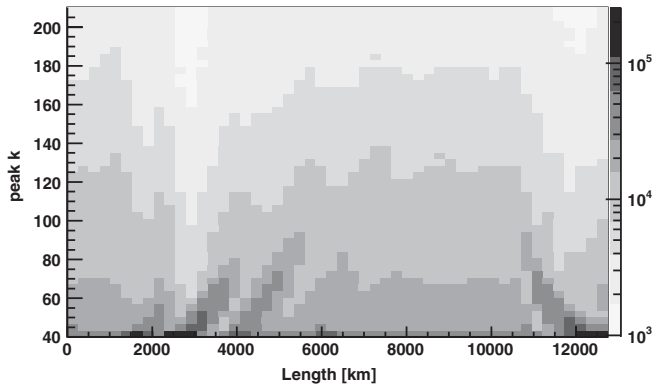

FIG. 15. Distribution of the position of the maximum peak in k as a function of matter-traversed path length L, assuming water Cherenkov energy resolution. There are 500 000 simulated supernovae per L, each with 60 000 events.

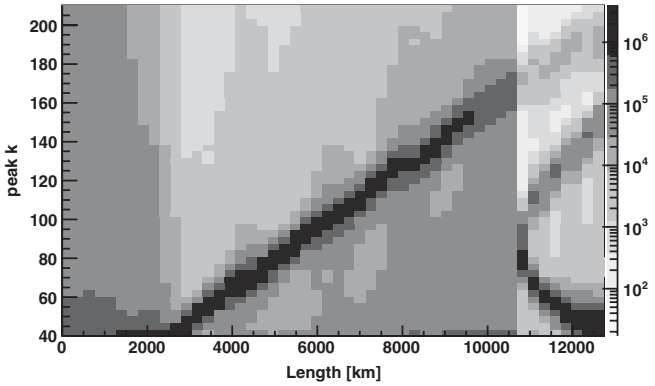

FIG. 16. Distribution of the position of the maximum peak in k as a function of matter-traversed path length L, assuming scintillator energy resolution. There are 5 000 000 simulated supernovae per L, each with 60 000 events.

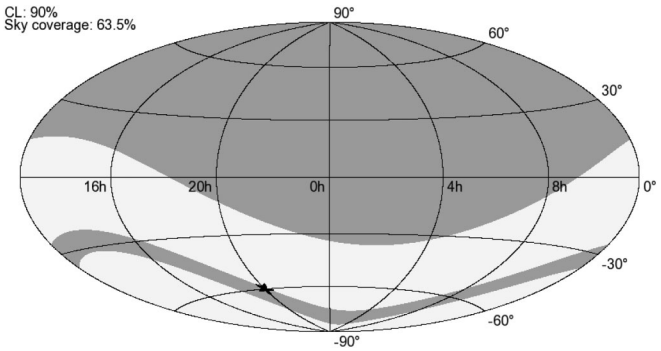

FIG. 17. Example scintillator sky map, for a single detector located in Finland, assuming a 60 000 event signal.

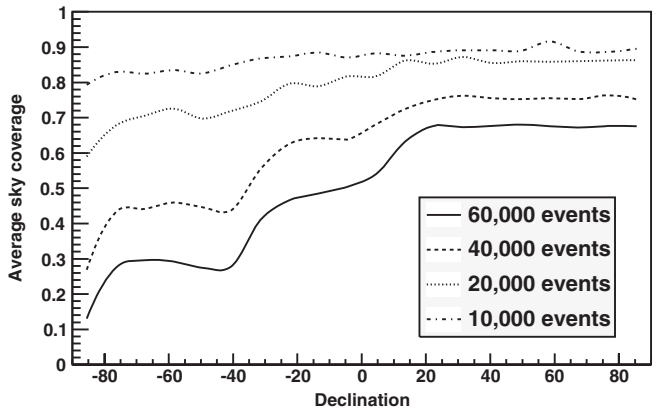

FIG. 18. Average scintillator sky coverage vs declination for a single detector located in Finland, for 10 000, 20 000, 40 000, and 60 000 event signals. In total 200 000 supernovae have been simulated for the 60 000 event case and 25 000 for the other cases.

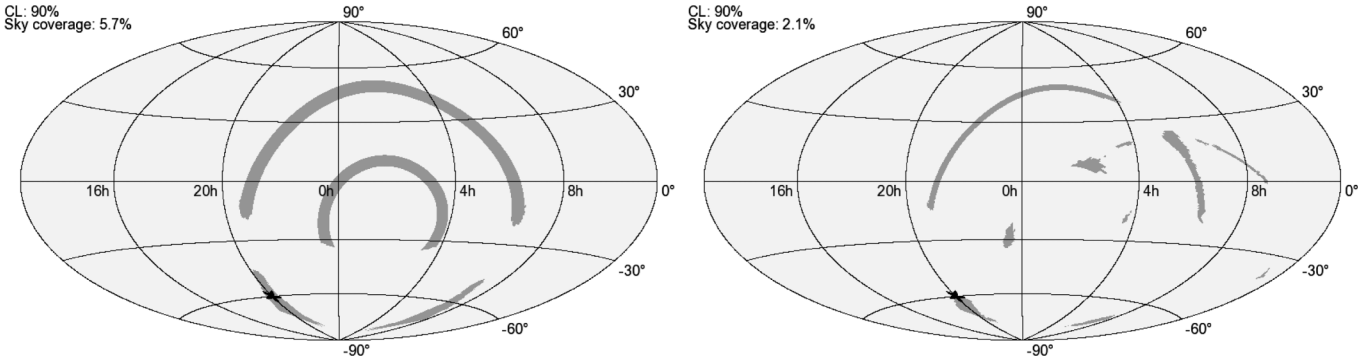

FIG. 19. Example scintillator sky maps, for a two (left panel) and three (right panel) detectors, each with a 60 000 event signal per detector.

Next we consider the case when multiple detectors are operating: Fig. 19 shows the results of combining the information from two and three scintillator detectors located in Finland, off the coast of Hawaii (19.72°N, 156.32°W), and South Dakota (44.45°N, 103.75°W). Figure 20 shows average sky coverage vs declination for these configurations.

3. Incorporating relative timing information

We consider briefly now the possibility of incorporating relative timing information between detectors to break degeneracies in the allowed region(s). A detailed study of the triangulation capabilities for specific neutrino signal and detector models is beyond the scope of this work. We instead do some back-of-the-envelope estimates based on those in Ref. [7]. For a signal registered in two detectors, the supernova direction can be constrained to a ring on the sky at angle θ with respect to the line between the detectors, with $\cos\theta = \Delta t/d$ and width $\delta(\cos\theta) \sim \frac{\delta(\Delta t)}{d}$, where d is the distance between the detectors and $\delta(\Delta t)$ is the time shift uncertainty between the pulses. We assume $\delta(\Delta t) \sim 30\ \mathrm{ms}/\sqrt{N_1}$, where N_1 is $\sim$1% of the total signal. A sharp feature in the signal timing could reduce $\delta(\Delta t)$.

Figure 21 shows an example for two detectors (located in Finland and Hawaii), with the time-triangulated allowed region superimposed: the intersection clearly narrows down the allowed directions.

We can imagine also that another, nonscintillator, neutrino detector (or even a gravitational wave detector, e.g., [40]) could provide relative timing information as well. For

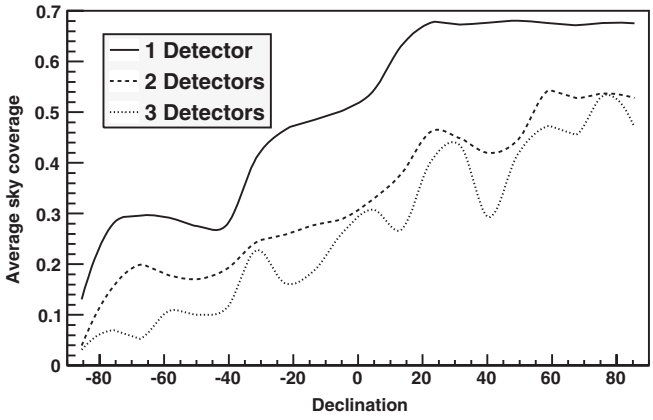

FIG. 20. Average scintillator sky coverage vs declination for one, two, and three detectors with 60 000 events each. For one detector 200 000 supernovae have been simulated, for two detectors the number is 3500 and for three detectors it is 1256.

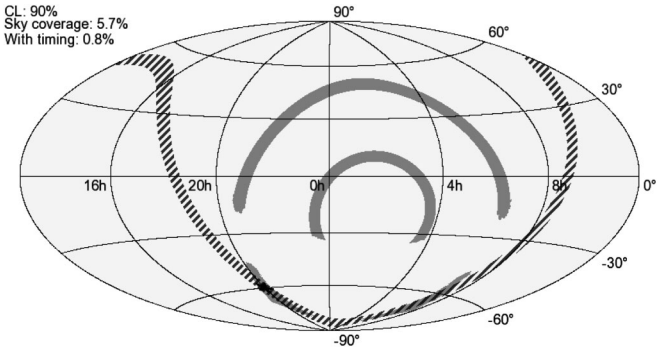

FIG. 21. Example two scintillator detector sky map, with estimate of allowed region based on relative timing information superimposed (striped band).

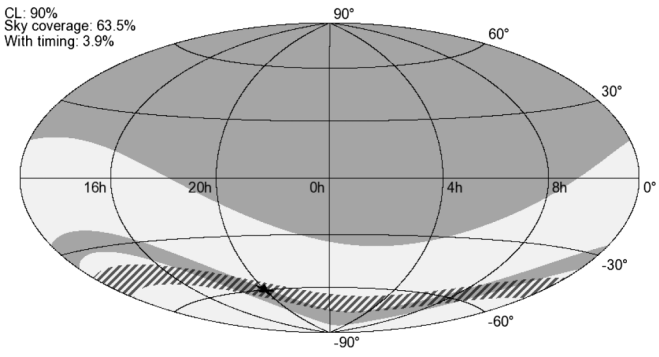

FIG. 22. Example single scintillator detector sky map, with estimated allowed region determined from relative timing with the IceCube signal (striped band).

example, IceCube at the South Pole could yield few ms timing [41]. Figure 22 shows an example of the intersection of the estimated IceCube plus single scintillator detector time-triangulation allowed region [assuming $\delta(\Delta t) \sim 1$ ms] with the single scintillator oscillation pattern region.

IV. DISCUSSION

We have assumed in these idealized scenarios perfect knowledge of oscillation parameters. In practice, imperfect knowledge of the oscillation parameters will create some uncertainties. In particular, the power spectrum peak position is sensitive to the value of Δm^2_{12}; the peak height is sensitive to both Δm^2_{12} and θ_{12}; θ_{13} also has an effect on both $k_{\rm peak}$ and h. (The oscillation pattern is quite insensitive to Δm^2_{23} and θ_{23}.) Figures 23 and 24 show the effect on $k_{\rm peak}$ and h values of varying the oscillation parameters within currently allowed ranges [42].

From these plots one can infer that $\lesssim 1\%$ knowledge of the mixing parameters is desirable. However, one can be quite optimistic that such precision will have been attained by the time a core collapse supernova happens when a large scintillator detector is running.

Another uncertainty that will affect the quality of pointing is that of the density of matter in the Earth. We found only small differences in $k_{\rm peak}$ and h from varying the mantle density by $\pm 3\%$, or from varying the overall density by $\pm 5\%$, but observed some changes in peak pattern for the case of neutrinos passing through the core when varying the core density by $\pm 10\%$.

We consider now the sensitivity of our results to the model we have chosen. We expect that the pointing uncertainty for a given measurement due to lack of knowledge of the neutrino spectrum will be small. The source of the directional information is the modulation of the spectrum: the modulation pattern depends on neutrino oscillation in the Earth and so should be rather insensitive to the incoming flux spectral parameters (see, also, Ref. [17]). Figure 25, showing the effect on $k_{\rm peak}$ of varying the parameters in the model of Eq. (1), supports this idea: only for the case of neutrinos traversing the core region (for which there is high sensitivity to small effects) is there a significant variation in the power spectrum largest peak position. In addition, for a real case the underlying neutrino flux and spectral shape will be measured with high statistics and hence the expected $k_{\rm peak}$ and h dependence on L can be computed from the data themselves.

We note that the *average* quality of pointing will depend somewhat on the model, since larger differences between $\bar{\nu}_x$ and $\bar{\nu}_e$ spectra will improve detectability of the power spectrum peaks [17]. Figure 26 gives examples of average coverage for three sets of neutrino spectrum parameters.

Many other effects may degrade the quality of direction information that can be obtained using this technique. There may be real spectral features (e.g., ''splits'') which introduce additional Fourier components that could mask the peak, and detector imperfections may do the same. We

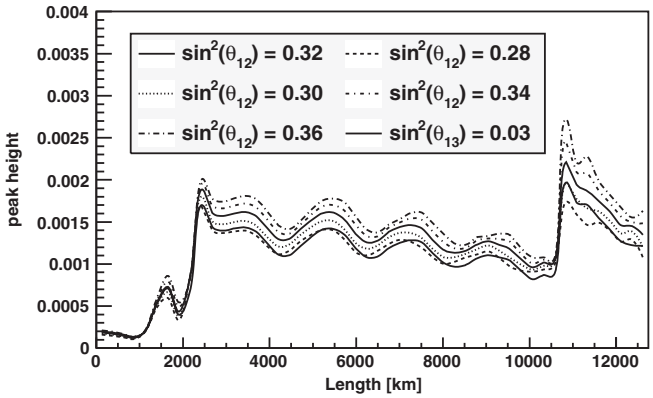

FIG. 24. Effect of varying θ_{12} and θ_{13} on the peak height as a function of L; in each case the other oscillation parameters are held at their nominal values.

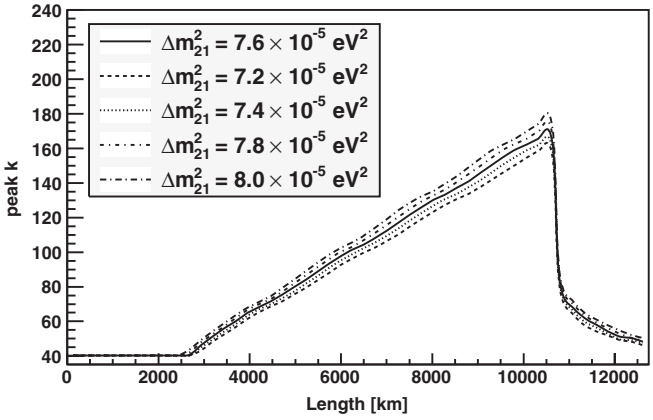

FIG. 23. Effect of varying Δm^2_{12} on the peak position as a function of L; in each case other oscillation parameters are held at their nominal values.

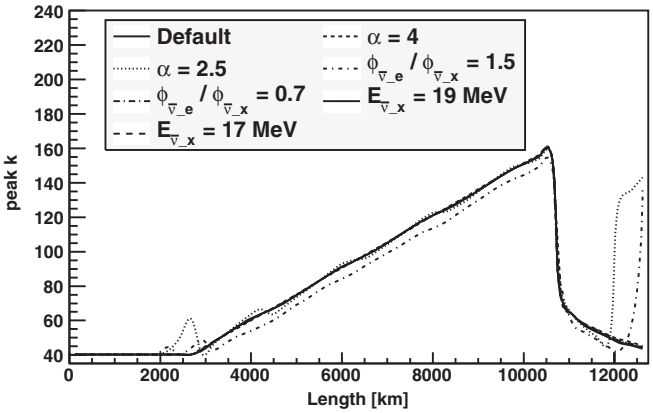

FIG. 25. Effect of varying model parameters on $k_{\rm peak}$. The default model is that described in Sec. III, and in each case one parameter is varied and the others held constant.

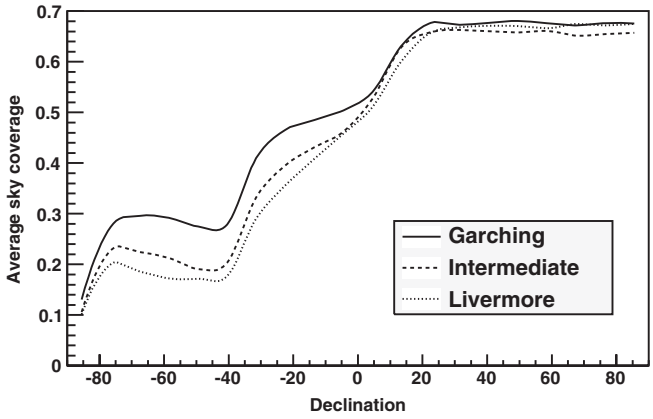

FIG. 26. Average scintillator sky coverage as a function of declination for three different neutrino spectrum models, for a 60 000 event signal observed in Finland. The ''Garching'' model is the default one described in Sec. III. The ''Livermore'' model ([17,44]) is described with parameters $\alpha = 3$, $\frac{\phi_{\bar{\nu}_e}}{\phi_{\bar{\nu}_x}} = 1.6$, and $E_{\bar{\nu}_x} = 24$ MeV. The ''intermediate'' model parameters are $\alpha = 3$, $\frac{\phi_{\bar{\nu}_e}}{\phi_{\bar{\nu}_x}} = 1.1$, and $E_{\bar{\nu}_x} = 20$ MeV. For the Garching model 200 000 supernovae were simulated, and 45 000 were simulated for the Livermore and intermediate ones.

acknowledge also that there may be practical difficulties with the rapid exchange of information between experimenters required for prompt extraction of directional information from multiple detectors. Nevertheless this technique represents an interesting possibility—even half the sky is better than no directional information. The oscillation pattern gives information about direction with even a single detector, and enhances any multiple-detector time-triangulation information. Even if information from only a single detector is available, or if there are significant ambiguities, one can imagine also looking at the intersection of the allowed region with the galactic plane regions for which supernovae are most likely to occur ([25]) (perhaps using the known probability distribution as a Bayesian prior) to improve the chances of finding the supernova; see Fig. 27.

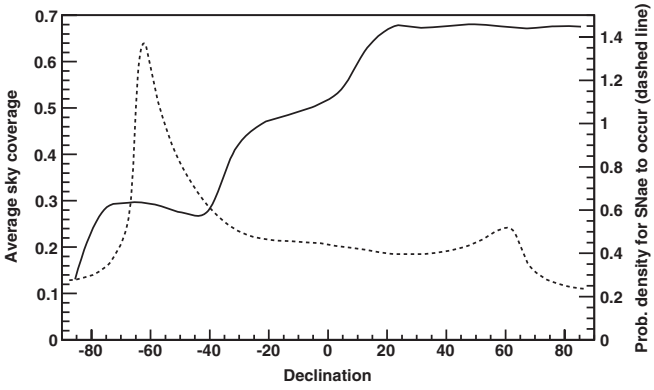

FIG. 27. Average scintillator sky coverage vs declination for a single detector in Finland, with the expected probability for supernova occurrence superimposed from Ref. [25].

We note that these estimates of pointing quality have been done using a fairly simple technique based on only two parameters characterizing the power spectra. One can imagine employing more sophisticated algorithms, e.g., making use of secondary peaks or matching to a template, and possibly incorporating knowledge of specific detector properties or neutrino flux spectral features. So although real conditions may degrade quality, with this simplified study we have not fully exploited all potentially available information.

As a final note: the technique could in principle work to determine directional information for neutrino signals from other astrophysical sources, such as black hole-neutron star mergers [43], assuming sufficient statistics.

V. SUMMARY

We have explored a technique by which neutrino detectors with good energy resolution can determine information about the direction of a supernova via measurement of the matter oscillation pattern. This method will only work for favorable (but currently allowed) oscillation parameters; it requires large statistics, good energy resolution, and well-known oscillation parameters, and it works best for relatively long neutrino path lengths through the Earth. The method is especially promising for scintillator detectors. The requirements will be fulfilled in optimistic but not inconceivable scenarios. The quality of direction information for a specific instance of a supernova neutrino measurement will depend on several factors: number of detected neutrinos, number of detectors, location of the supernova with respect to the detectors, and the neutrino flavor-spectral composition. Figure 18 summarizes average sky coverage for a single scintillator detector. Combining information from multiple detectors, and possibly incorporating relative timing information, may provide significant improvement. Figure 20 summarizes potential improvement for multiple detectors.

The matter oscillation pointing method is inferior to that using elastic scattering in imaging Cherenkov (or argon time projection chamber) detectors; elastic scattering remains the best bet for pointing to the supernova. However it is possible that a supernova will occur when no such detector is running, in which case one should use whatever directional information can be extracted from the observed signals.

ACKNOWLEDGMENTS

The research activities of K. S. and R. W. are supported by the U.S. Department of Energy and the National Science Foundation. A. B. was supported for work at Duke University by the Deutscher Akademischer Austausch Dienst summer internship program.

[1] K. Scholberg, arXiv:astro-ph/0701081.
[2] J. Appel *et al.*, Physics with a High Intensity Proton Source at Fermilab (2008), http://www.fnal.gov/directorate/Longrange/Steering_Public/P5/GoldenBook-2008-02-03.pdf.
[3] K. Nakamura, Int. J. Mod. Phys. A **18**, 4053 (2003).
[4] A. de Bellefon *et al.*, arXiv:hep-ex/0607026.
[5] T. Marrodan Undagoitia *et al.*, J. Phys. Conf. Ser. **120**, 052018 (2008).
[6] J. G. Learned, S. T. Dye, and S. Pakvasa, arXiv:0810.4975.
[7] J. F. Beacom and P. Vogel, Phys. Rev. D **60**, 033007 (1999).
[8] R. Tomas *et al.*, Phys. Rev. D **68**, 093013 (2003).
[9] P. Vogel and J. F. Beacom, Phys. Rev. D **60**, 053003 (1999).
[10] M. Ikeda *et al.* (Super-Kamiokande Collaboration), Astrophys. J. **669**, 519 (2007).
[11] F. Halzen, J. E. Jacobsen, and E. Zas, Phys. Rev. D **53**, 7359 (1996).
[12] This technique was studied for a gadolinium-loaded scintillator in Refs. [13,14]; however gadolinium loading for future large scintillator detectors does not seem to be planned.
[13] M. Apollonio *et al.* (CHOOZ Collaboration), Phys. Rev. D **61**, 012001 (1999).
[14] K. A. Hochmuth, M. Lindner, and G. G. Raffelt, Phys. Rev. D **76**, 073001 (2007).
[15] H. Watanabe, Toward Low Energy Antineutrinos Directional Measurement, http://cdsagenda5.ictp.trieste.it/askArchive.php?base=agenda&categ=a08170&id=a08170s13t21/lecture_notes (2009).
[16] A. S. Dighe, M. T. Keil, and G. G. Raffelt, J. Cosmol. Astropart. Phys. 06 (2003) 006.
[17] A. S. Dighe, M. Kachelriess, G. G. Raffelt, and R. Tomas, J. Cosmol. Astropart. Phys. 01 (2004) 004.
[18] A. S. Dighe and A. Y. Smirnov, Phys. Rev. D **62**, 033007 (2000).
[19] C. Lunardini and A. Y. Smirnov, Nucl. Phys. **B616**, 307 (2001).
[20] K. Takahashi and K. Sato, Phys. Rev. D **66**, 033006 (2002).
[21] C. Lunardini and A. Y. Smirnov, J. Cosmol. Astropart. Phys. 06 (2003) 009.
[22] B. Dasgupta, A. Dighe, and A. Mirizzi, Phys. Rev. Lett. **101**, 171801 (2008).
[23] A. Dighe, J. Phys. Conf. Ser. **136**, 022041 (2008).
[24] S. T. Dye, Phys. Lett. B **679**, 15 (2009).
[25] A. Mirizzi, G. G. Raffelt, and P. D. Serpico, J. Cosmol. Astropart. Phys. 05 (2006) 012.
[26] Large liquid argon detectors will also have supernova neutrino sensitivity [27]. Such detectors are primarily sensitive to ν_e rather than $\bar{\nu}_e$; they have good energy resolution and in principle could employ the matter oscillation pointing technique for the case when mixing parameters favor ν_e oscillation in the Earth. However liquid argon time projection chambers also have excellent intrinsic pointing capability, and the angular resolution for neutrino-electron elastic scattering will certainly be superior. Therefore we will not consider liquid argon further here.
[27] A. Bueno, I. Gil Botella, and A. Rubbia, arXiv:hep-ph/0307222.
[28] G. G. Raffelt, M. T. Keil, R. Buras, H.-T. Janka, and M. Rampp, arXiv:astro-ph/0303226.
[29] B. Dasgupta, A. Dighe, G. G. Raffelt, and A. Y. Smirnov, Phys. Rev. Lett. **103**, 051105 (2009).
[30] R. Wendell (2009), http://www.phy.duke.edu/~raw22/public/Prob3++/.
[31] A. Dziewonski and D. Anderson, Phys. Earth Planet. Inter. **25**, 297 (1981).
[32] V. Barger *et al.*, Phys. Rev. D **22**, 2718 (1980).
[33] C. Amsler *et al.* (Particle Data Group), Phys. Lett. B **667**, 1 (2008).
[34] K. Eguchi *et al.* (KamLAND Collaboration), Phys. Rev. Lett. **90**, 021802 (2003).
[35] M. Aglietta *et al.*, Nuovo Cimento Soc. Ital. Fis. A **105**, 1793 (1992).
[36] N. Y. Agafonova *et al.*, Astropart. Phys. **27**, 254 (2007).
[37] L. Cadonati, F. P. Calaprice, and M. C. Chen, Astropart. Phys. **16**, 361 (2002).
[38] C. Kraus (SNO+ Collaboration), Prog. Part. Nucl. Phys. **57**, 150 (2006).
[39] G. V. Domogatsky, V. I. Kopeikin, L. A. Mikaelyan, and V. V. Sinev, Phys. At. Nucl. **70**, 1081 (2007).
[40] G. Pagliaroli, F. Vissani, E. Coccia, and W. Fulgione, Phys. Rev. Lett. **103**, 031102 (2009).
[41] F. Halzen and G. G. Raffelt, Phys. Rev. D **80**, 087301 (2009).
[42] S. Abe *et al.* (KamLAND Collaboration), Phys. Rev. Lett. **100**, 221803 (2008).
[43] O. L. Caballero, G. C. McLaughlin, and R. Surman, Phys. Rev. D **80**, 123004 (2009).
[44] T. Totani, K. Sato, H. E. Dalhed, and J. R. Wilson, Astrophys. J. **496**, 216 (1998).